Bifurcation Behavior and Efficient Pure Hydrogen Production for Fuel Cells Using a Novel Autothermic Membrane Circulating Fluidized-Bed (CFB) Reformer: Sequential Debottlenecking and the Contribution of John Grace

Zhongxiang Chen and Said S. E. H. Elnashaie*

Department of Chemical Engineering, Auburn University, Auburn, Alabama 36849-5127

I am pleased to contribute, together with my Ph.D. student Zhongxiang Chen, this paper to the *Ind. Eng. Chem. Res.* special issue for Professor John Grace of the University of British Columbia in recognition of his many contributions to subjects of interest to readers in this journal. I have known John since the early 1970s (over 30 years now) when we were both studying for our Ph.D.'s in the U.K. (he was in Cambridge, and I was in Edinburgh). Since then, we have always been in close contact. I visited him at McGill and British Columbia Universities, and he visited me at King Saud and Auburn Universities, and we cooperated in the development of novel fluidized-bed reformers (e.g., Adris, A.; Grace, J.; Lim, C.; Elnashaie, S. S. E. H. Fluidized Bed Reaction System for Steam Hydrocarbon Gas Reforming to Produce Hydrogen. U.S. Patent 5,326,550, Jun 1994; Canadian Patent 2,081,170, Dec 2002). This was our first explicit application of the sequential debottlenecking methodology, although John has used the approach implicitly in many cases to develop novel processes. He is running the Fluidization Research Center (FRC), which he established in 1997 at the University of British Columbia (UBC) and which is funded by Mitsubishi Chemical Corporation (MCC), the Natural Science and Engineering Research Council of Canada (NSERC), and a number of other government and industrial sponsors. The contributions of Professor Grace to fluidization and fluidized-bed reactors are outstanding. Recently, he edited the excellent proceedings for the 7th International Conference on Circulating Fluidized Beds, Niagara Falls, Ontario, Canada, May 5−8, 2003, and contributed excellent papers to it. I would like to congratulate John for his latest award of the Innovation and Science Council of British Columbia for 2003. He was accorded this prestigious award for distinguishing himself—as an educator, researcher, and innovator—in his 35-year career as a leading authority on fluidization and chemical reaction engineering. I would like also to congratulate him for his recovery from his latest operation and wish him a fast and safe complete recovery. If you want to know more about the outstanding achievements of Professor John Grace, I advise you to visit his Web site at the University of British Columbia, Canada (http://faculty.chml.ubc.ca/jgrace/). The present paper is an investigation of the bifurcation behavior of a novel circulating fluidized-bed (CFB) autothermic reformer. I have learned a lot about CFBs from the excellent work of Professor John Grace. My Ph.D. student Zhongxiang Chen and I are happy to contribute this paper to this special IECR issue in the honor of this excellent academician.

—Said S. E. H. Elnashaie

The multiplicity of steady states (static bifurcation behavior, SBB) in a novel circulating fluidized-bed (CFB) membrane reformer for the efficient production of hydrogen by steam reforming of heptane (model component of heavy hydrocarbons) is investigated. The present paper highlights the practical implications of this phenomenon on the behavior of this novel reformer with a special focus on hydrogen production. Two configurations are considered and compared. One has catalyst regeneration before gas−solid separation, and the other has catalyst regeneration after gas−solid separation. The multiplicity of the steady states prevails over ranges of a number of design and operating parameters with significant impacts on the performance of the reformer. The basis of process evaluation is focused on the net hydrogen production. The dependence of the behavior of this autothermal CFB is shown to be quite complex and to defy the simple logic of nonautothermal processes. The unit can be a very efficient hydrogen producer provided that its bifurcation behavior is well understood and correctly exploited.

Introduction

Currently, hydrogen is receiving incresing attention as a promising clean fuel for the future.[1,2] Steam reforming of hydrocarbons is the most prominent process for hydrogen production,[3−7] which extracts hydrogen not only from hydrocarbons but also from water. The classical reactor for hydrogen production is the fixed-bed steam reformer (first-generation reformer, FGR), which is inefficient; highly polluting; and suffers from catalyst deactivation, especially when using higher hydrocarbons as a feedstock.[5,8−10] Over the past decade, significant progress has been made toward overcoming the limitations of conventional fixed-bed reforming

* To whom correspondence should be addressed. E-mail: nashaie@eng.auburn.edu. Fax: 334-887-3905

10.1021/ie0341799 CCC: $27.50
Published on Web 03/02/2004

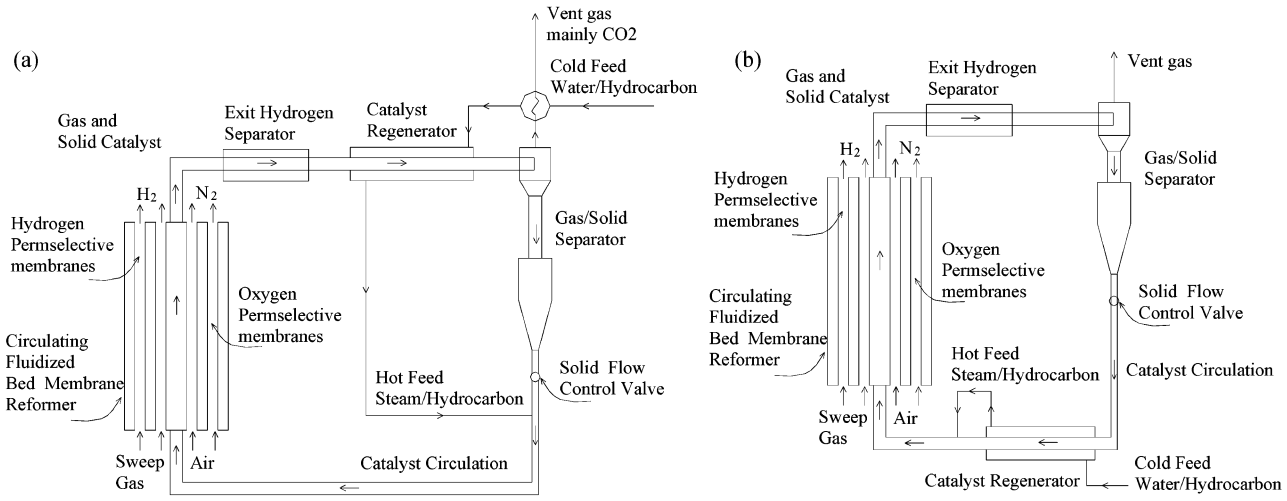

Figure 1. Schematic of the circulating reactor−regenerator membrane reformer: (a) catalyst regeneration is carried out before gas−solid separation, and (b) catalyst regeneration is carried out after gas−solid separation.

systems. Various alternatives tested have included fixed beds with hydrogen permselective membranes,[11−14] microchannel reformers for hydrogen production from natural gas,[15] and catalytic oxidative steam reforming.[16,17] Further advancements were made by moving to a bubbling fluidized-bed reformer with hydrogen permselective membranes (BFBMR),[18−24] which we refer to here as the second-generation reformer (SGR). This technology has been actively carried forward by Professor John Grace, and a company (MRT) has been formed to commercialize this technology. This technology has been the most successful milestone to date and is a proven success for natural gas. Recently, a novel circulating fluidized-bed (CFB) membrane reformer that can use a wide range of hydrocarbons, including natural gas, naphtha, gasoline, diesel, heavy hydrocarbons, and even bio-oils from biomass or municipal solid waste, has been shown to be efficient and flexible for the production of pure hydrogen.[7,25−28] This technology is referred to as the third-generation reformer (TGR). Development from the FGR to the SGR and relatively recently to the present TGR is based on what can be called sequential debottlenecking, which relies on the simple fact that the limited productivity of any process is caused by certain bottleneck(s). These bottlenecks can arise from the reaction rate, mass-transfer rate, heat-transfer rate, hydrodynamic limitations, etc., or a nonlinear coupling between two or more of these bottlenecks. This issue dictates an intradisciplinary research approach, which is one of the research basis for cooperation between Grace and Elnashaie groups.[20,23] FGRs suffer from a large number of limitations (bottlenecks), the main one of which is the intraparticle diffusion resistance of the catalyst pellets, giving rise to very low effectiveness factors, $\eta = 10^{-2}-10^{-3}$.[5,8,9] The SGR was developed to break all of these limitations (debottlenecking); however, new bottlenecks were created with this configuration because there are inherent hydrodynamic limitation associated with the SGR, in addition to thermal and other limitations.[7,25−28] The TGR is a novel configuration that will be more efficient than both the FGR and the SGR.[7,25−28]

In this paper, bifurcation behavior during the efficient production of pure hydrogen for fuel cells in this novel TGR formed of an autothermic CFB membrane reformer is explored in some detail for two configurations. As shown in Figure 1, in the first configuration, catalyst regeneration is carried out before gas−solid separation (Figure 1a), whereas in the second configuration, it is carried out after gas−solid separation (Figure 1b). A number of palladium-based hydrogen permselective membranes for hydrogen removal and dense perovskite oxygen permselective membranes for the introduction of oxygen for oxidative reforming in the riser reformer are available. Heptane is used as a model component of heavy hydrocarbons. For the efficient production of pure hydrogen, the gases and solids from the riser reformer (for both configurations) enter an exit hydrogen separator for the further removal of any remaining hydrogen. For the first configuration, shown in Figure 1a, the carbon deposited on the nickel reforming catalyst is burned off by excess air in the catalyst regenerator, as are flammable gases such as hydrocarbons (unreacted heptane and byproduct methane) and carbon monoxide. The regenerated catalyst is separated from the gases using a gas−solid separator and then recycled to the riser reformer. In contrast, for the second configuration, shown in Figure 1b, the solid catalyst is first separated from the gases, and then the carbon deposited on the nickel reforming catalyst is burned off by excess air in the catalyst regenerator, after which the regenerated catalyst is separated from the carbon dioxide. Exit hydrocarbons (unreacted heptane and byproduct methane) and carbon monoxide are used together with carbon dioxide from the catalyst regenerator as part of the feed to a novel dry reformer.[28] Regenerated catalyst is recycled to the riser reformer. For minimum energy consumption in this novel TGR, the heat of reaction(s) occurring in the catalyst regenerator is utilized to preheat the cold feed water (to generate steam) and hydrocarbon, as well as the recycled catalyst. Bifurcation behavior is investigated when autothermal operation of this reactor−regenerator configuration is achieved. That is, under autothermic reformer operations, the heat generated in the adiabatic catalyst regenerator is equal to the heat consumed in the adiabatic endothermic steam reformer, which is supplied by preheating of the cold feed water and hydrocarbon, as well as the recycled catalyst. This configuration has some resemblence to modern fluid catalytic cracking (FCC) units.[29]

Reaction Scheme and Kinetics

Table 1 summarizes the reactions and kinetics used for the simulation of this novel autothermic CFB

Table 1. Reactions and Kinetics Rate Equations for the Reformer−Regenerator System

(a) Reactions and Kinetic Rate Equations in the Riser Reformer

reaction	kinetic rate equation[a]	ref
$C_7H_{16} + 7H_2O \rightarrow 7CO + 15H_2$	$r_1 = \dfrac{k_1 P_{C_7H_{16}}}{\left(1 + 25.2\dfrac{P_{C_7H_{16}} P_{H_2}}{P_{H_2O}} + 0.077\dfrac{P_{H_2O}}{P_{H_2}}\right)^2}$	3
$CO + 3H_2 \rightleftharpoons CH_4 + H_2O$	$r_2 = k_2\left(\dfrac{P_{CO} P_{H_2}^{0.5}}{K_2} - \dfrac{P_{CH_4} P_{H_2O}}{P_{H_2}^{2.5}}\right)\Big/ \mathrm{DEN}^2$	4
$CO + H_2O \rightleftharpoons CO_2 + H_2$	$r_3 = k_3\left(\dfrac{P_{CO} P_{H_2O}}{P_{H_2}} - \dfrac{P_{CO_2}}{K_3}\right)\Big/ \mathrm{DEN}^2$	4
$CH_4 + 2H_2O \rightleftharpoons CO_2 + 4H_2$	$r_4 = k_4\left(\dfrac{P_{CH_4} P_{H_2O}^{2}}{P_{H_2}^{3.5}} - \dfrac{P_{CO_2} P_{H_2}^{0.5}}{K_2 K_3}\right)\Big/ \mathrm{DEN}^2$	4
$C_7H_{16} + 3.5O_2 \rightarrow 7CO + 8H_2$	$r_5 = k_5 T P^{0.3} C_{C_7H_{16}}^{0.5} C_{O_2}$	30
$CH_4 + 2O_2 \rightarrow CO_2 + 2H_2O$	$r_6 = k_6 P_{CH_4} P_{O_2}$	31
$CH_4 + CO_2 \rightleftharpoons 2CO + 2H_2$	$r_7 = k_7 P_{CH_4} P_{CO_2}\left(1 - \dfrac{P_{CO}^{2} P_{H_2}^{2}}{K_7 P_{CH_4} P_{CO_2}}\right)$	31
$C_7H_{16} \rightarrow 7C + 8H_2$	$r_8 = k_8 P_{C_7H_{16}}^{0.569}$ [b]	32
$CH_4 \rightleftharpoons C + 2H_2$	$r_9 = \dfrac{k_9 K_{CH_4}\left(P_{CH_4} - \dfrac{P_{H_2}^{2}}{K_{9a}}\right)}{\left(1 + \dfrac{P_{H_2}^{1.5}}{K_{9b}} + K_{CH_4} P_{CH_5}\right)^2}$	33
$2CO \rightarrow C + CO_2$	$r_{10} = \dfrac{k_{10} P_{CO}}{\left(1 + K_{10a} P_{CO} + K_{10b}\dfrac{P_{CO_2}}{P_{CO}}\right)^2}$	34
$C + H_2O \rightarrow CO + H_2$	$r_{11} = k_{11} P_{H_2O}^{0.5}$	35
$C + 0.5O_2 \rightarrow CO$	$r_{12} = k_{12} P_{O_2}^{0.5}$	35
$C + CO_2 \rightarrow 2CO$	$r_{13} = k_{13} P_{CO_2}^{0.5}$	35

(b) Reactions and Heats of Reaction in the Catalyst Regenerator

reaction	heat of combustion $\Delta H°$ (kJ/mol)
$C_7H_{16} + 11O_2 \rightarrow 7CO_2 + 8H_2O$	−4501.48[c]
$CH_4 + 2O_2 \rightarrow CO_2 + 2H_2O$	−802.76[c]
$CO + 0.5O_2 \rightarrow CO_2$	−282.98
$C + O_2 \rightarrow CO_2$	−393.51

[a] Where $\mathrm{DEN} = 1 + K_{CO}P_{CO} + K_{H_2}P_{H_2} + K_{CH_4}P_{CH_4} + K_{H_2O}P_{H_2O}/P_{H_2}$. [b] Empirically obtained from the experimental data reported by Rostrup-Nielsen.[32] [c] Water is in the vapor state.

membrane reformer−regenerator system (TGR). Because there are two possible configurations for catalyst regeneration, namely, location of the catalyst regenerator before or after the gas−solid separator, the reactions in the catalyst regenerator are different. For the first case, shown in Figure 1a, four reactions listed in Table 1b take place in the catalyst regenerator, whereas for the second case, shown in Figure 1b, only carbon burning (the last reaction in Table 1b) takes place in the catalyst regenerator.

Modeling of the Complete Circulating System

Unless otherwise specified, it is assumed that the reaction(s) in the catalyst regenerator is (are) highly efficient (or that the catalyst regenerator is overdesigned) so that we can consider these reactions (the burning of carbon, unreacted hydrocarbons, and carbon monoxide) to be complete. Therefore, during the modeling of the CFB membrane reformer, only heat produced in the catalyst regenerator due to complete conversion and its thermal effects on the whole system are considered. The riser reformer is modeled as a plug-flow reactor with no gas−solid slip because of the large gas velocity (typical ∼3 m/s) and the use of fine catalyst particles (186 μm).[36] The other main assumptions for the CFB membrane reformer/regenerator are as follows: (1) Operation is at steady state. (2) No hydrogen oxidation takes place over the nickel reforming catalyst in the reformer. (3) The palladium-based hydrogen membranes and dense perovskite oxygen membranes are 100% selective for the permeation of the components hydrogen and oxygen, respectively. (4) The heat capacities of the components and the heats of reaction are constant. (5) The pressures in the riser reformer and hydrogen and oxygen membrane tubes are constant. (6) The hydrogen and oxygen permselective membranes are not affected by carbon deposition. (7) To produce hydrogen efficiently, the hydrogen remaining in the exit stream of the riser reformer is further fully separated in an exit hydrogen separator before entering the catalyst regenerator. (8) The heat of reaction(s) occurring in the catalyst regenerator is used to preheat the cold feed water (to generate steam), heptane, and the catalyst before recycling to the riser reformer, in which the necessary heat for the endothermic steam reforming

Table 2. Steady-State Equations for the CFB Membrane Reformer

	Material Balance in the Riser Reformer Reaction Side
component i	$\frac{dF_i}{dl} = \rho_C(1-\epsilon)A_f\sum_{j=1}^{13}\sigma_{i,j}r_j - aJ_{H_2}\pi N_{H_2}d_{H_2} + bJ_{O_2}\pi N_{O_2}d_{O_2}$
	for $i = C_7H_{16}$, CH_4, CO_2, CO, H_2, H_2O, O_2, and C with $\begin{cases} a=1, b=0 & \text{for } i = H_2 \\ a=0, b=1 & \text{for } i = O_2 \\ a=0, b=0 & \text{for } i \neq H_2 \neq O_2 \end{cases}$
boundary condition	at $l = 0$, $F_i = F_{i0}$
	Material Balance in the Hydrogen Permselective Membrane Tubes
hydrogen	$\frac{dF_{H_2,P}}{dl} = J_{H_2}\pi N_{H_2}d_{H_2}$
boundary condition	at $l = 0$, $F_{H_2,P} = F_{H_2,P0} = 0$
sweep gas	$F_{SG,P} = F_{SG,P0} = \text{constant}$
hydrogen permeation flux[38]	$J_{H_2} = \frac{Q_{H_2}}{\delta_{H_2}}\exp\left(\frac{-E_{H_2}}{RT}\right)(\sqrt{p_{H_2,r}} - \sqrt{p_{H_2,p}})$
	Material Balance in the Oxygen Permselective Membrane Tubes
oxygen	$\frac{dF_{O_2,P}}{dl} = -J_{O_2}\pi N_{O_2}d_{O_2}$
boundary condition	at $l = 0$, $F_{O_2,P} = F_{O_2,P0}$
nitrogen (in air)	$F_{N_2,P} = F_{N_2,P0} = \text{constant}$
oxygen permeation flux[39]	$J_{O_2} = Q_{O_2}\exp\left(\frac{-E_{O_2}}{RT}\right)\frac{T}{\delta_{O_2}}\ln\left(\frac{P_{O_2,p}}{P_{O_2,r}}\right)$
	Energy Balance in the Riser Reformer and Membrane Tubes
temperature profile	$\frac{dT}{dl} = \frac{\sum_{j=1}^{13} r_j(-\Delta H_j)\rho_C(1-\epsilon)A_f + \dot{Q}}{\sum F_i C_{pi}}$
boundary condition	at $l = 0$, $T = T_0$
	Catalyst Deactivation and Modified Reaction Kinetics[26]
specific catalyst activity	$\phi_j = \begin{cases} \exp(-\alpha_C C_k) & \text{if reaction } j \text{ is affected by carbon deposition} \\ 1.0 & \text{if reaction } j \text{ is not affected by carbon deposition} \end{cases}$
reaction rate	$r_j = r_{j0}\phi_j$
	Energy Balance in the Catalyst Regenerator
heat generation rate	$Q_g = \begin{cases} \sum_{j=14}^{17} F_{ii}(-\Delta H_j) & \text{if catalyst regeneration is before gas−solid separation} \\ & (ii = C_7H_{16}, CH_4, \text{CO, and C}) \\ F_C(-\Delta H_{17}) & \text{if catalyst regeneration is after gas−solid separation} \end{cases}$
preheating rate	$Q_P = \sum F_k[(T_{k,b} - T_{room})C_{pk(l)} + \Delta H_{k,vap} + (T' - T_{k,b})C_{pk,b(g)}] + G_{cat}C_{pcat}(T' - T_{exit})$ (k = feed H_2O and C_7H_{16})
	Autothermal Reactor−Regenerator Membrane Reformer
autothermal system	$T_0 = T'$ and $Q_g = Q_P$

reactions is supplied. (9) The efficiency of the gas−solid separator is 100%.

The steady-state material and energy balance equations for this novel TGR are summarized in Table 2.

On the basis of these reaction kinetics (Table 1) and model equations (Table 2), the bifurcation behavior of this novel TGR is investigated. Unless otherwise specified, the investigation is performed using a series of standard parameters and reaction conditions as listed in Table 3. Note that, under autothermal operation, the feed temperature to the riser reformer is a system variable rather than a feed parameter. The method developed by Kunii and Levenspiel[37] is used to verify that the riser reformer is operating in the circulating fluidization regimes (fast fluidization or pneumatic transport regimes). The hydrogen yield is defined as the total number of moles of hydrogen produced per mole of heptane fed. Because there is no requirement for external heat supply under autothermal operation, the hydrogen yield is also the net hydrogen yield. The catalyst activity in Table 2 is defined as the ratio of the catalytic reaction rate to the initial reaction rate with fresh catalyst. Chen et al.[26] developed the exponential catalyst deactivation equation in Table 2 for calculating catalyst activity on the basis of a random carbon deposition mechanism on the nickel reforming catalyst.

Results and Discussion

Bifurcation Behavior When Catalyst Regeneration Is before Gas−Solid Separation. This is the configuration shown in Figure 1a, which is expected to give higher heat generation in the catalyst regenerator. As shown in Figure 1a, to produce pure hydrogen efficiently, the gas and solid mixture exiting from the riser reformer enters an exit hydrogen separator for the further removal of any remaining hydrogen.

Effects of Steam-to-Carbon Feed Ratio. For the entire bifurcation study, the standard simulation parameters and reaction conditions are those listed in Table 3 unless otherwise specified. Figure 2a−d shows the bifurcation results when the steam-to-carbon (S/C) feed ratio is used as the bifurcation parameter. The total gas flow rate is kept constant, and the flow rates of steam and heptane are modified according to the different steam-to-carbon feed ratios. Note that, in this autothermal system, the temperature of the feed to the reformer is a system variable rather than an external parameter. Bifurcation points are at S/C feed ratios of 1.444 and 2.251 mol/mol. The multiple steady states in this region are always classified into lower, middle, and upper steady states according to the reformer feed temperature (Figure 2a). When the S/C feed ratio is higher than 2.251 mol/mol, the autothermal circulating

Table 3. Standard Parameters and Reaction Conditions for the Bifurcation Investigation

Riser Reformer Construction Parameters	
length of riser reformer and membrane tubes	2 m
outside diameter of the reformer tube[5]	0.1154 m
wall thickness of the riser reformer[5]	0.0088 m
outside diameter of palladium-based hydrogen membrane tubes[21]	0.00498 m
wall thickness of palladium-based hydrogen membrane tubes [21]	0.00024 m
thickness of palladium layer on hydrogen membrane tubes[38]	20 μm
number of hydrogen membrane tubes	20
outside diameter of oxygen membrane tubes	0.00489 m
thickness of dense perovskite film on oxygen membrane tubes[40]	50 μm
number of oxygen membrane tubes	80
Nickel Steam Reforming Catalyst	
catalyst particle density[5]	2835 kg/m^3
mean diameter of catalyst particles[21]	186 μm
solid fraction of circulating fluidization bed[37,41]	0.2
Process Feeds and Reaction Conditions[3]	
feed flow rate of heptane	0.64 kmol/h
feed flow rate of steam	9 kmol/h
feed flow rate of hydrogen	0.1 kmol/h
steam-to-carbon feed ratio for the first configuration[a]	2 mol/mol
steam-to-carbon feed ratio for the second configuration	1 mol/mol
reaction pressure	1013 kPa
feed flow rate of sweep gas (steam) in hydrogen membrane tubes	1 kmol/h
operating pressure in palladium-based hydrogen membrane tubes	101.3 kPa
feed flow rate of air in oxygen membrane tubes	10 kmol/h
operating pressure in oxygen membrane tubes	3039 kPa

[a] First configuration has the catalyst regenerator before the gas−solid separator. [a] Second configuration has the catalyst regenerator after the gas−solid separator.

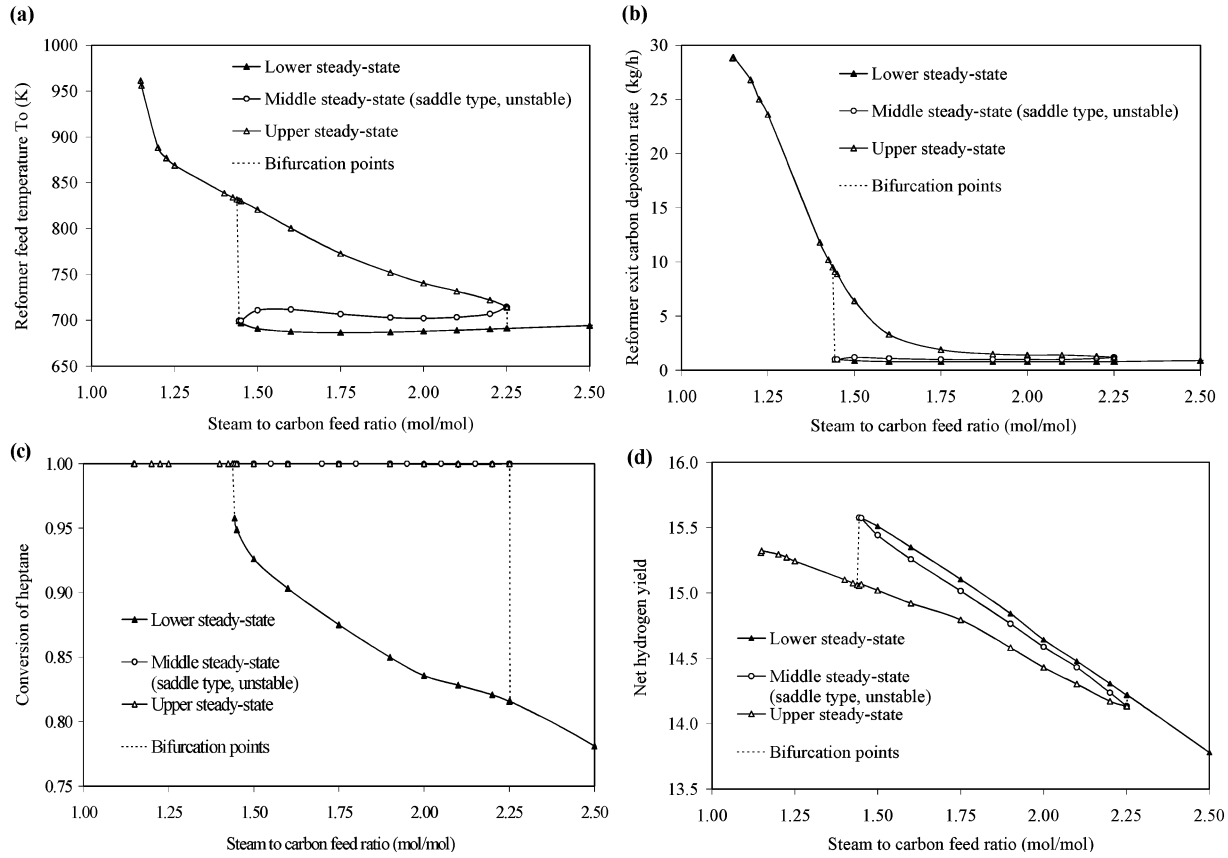

Figure 2. Bifurcation behavior with the team-to-carbon feed ratio as the bifurcation parameter in the autothermic CFB membrane reformer when catalyst regeneration is before gas−solid separation

feed temperatures are almost constant for changing S/C feed ratio. This is due to the fact that the higher the steam feed, the higher the extents of the endothermic steam reforming (of heptane and methane) and water−gas shift reactions, and the lower the carbon formation. To keep the system operating autothermally, the conversion of heptane has to be low so that enough fuel is provided to generate heat in the catalyst regenerator to supply the necessary heat for the endothermic steam reforming in the riser reformer. As a result, the autothermal temperature of the feed circulating to the riser reformer is the lowest, and the conversion of heptane is low. For example, at a steam-to-carbon feed ratio of 2.5 mol/mol, the conversion of heptane is 78.11%, the

net carbon deposition rate is 0.9 kg/h, and the autothermal circulating feed temperature is 694.31 K. Because the net hydrogen yield is defined as the amount of hydrogen produced per mole of heptane fed, the more the feed heptane is burned in the regenerator, the smaller the net hydrogen yield (Figure 2d). For example, at the high S/C feed ratio of 2.5 mol/mol, the net hydrogen yield is 13.78 mol of hydrogen per mole of heptane fed. When the S/C feed ratio is between 1.444 and 2.251 mol/mol, multiple steady states occur. For example, at a steam-to-carbon feed ratio of 2.0 mol/mol, three steady states exist with circulating reformer feed temperatures of 687.99, 702.15, and 740.34 K. Figure 2c shows that, for the middle and upper steady states, the conversion of heptane is 100%, whereas for the lower steady state, the conversion of heptane is between 81.6 and 95.80%. The conversion of heptane decreases as the S/C feed ratio is increased. This is opposite to the usual operation, where the performance improves as the S/C feed ratio is increased. However, in this autothermal system, a high S/C feed ratio prevents carbon formation, causing the heat supplied by the burning of carbon to decrease and forcing the system to a lower conversion. Fortunately, because of the large mass flow ratio of catalyst to gases and the continuous catalyst regeneration, the catalyst activity is kept high (>0.985), even at the low S/C feed ratio of 1.1475 mol/mol. In the multiplicity range of the S/C feed ratio, the higher the carbon deposition rate, the higher the autothermal temperature of the feed to the reformer. The trend for the hydrogen yield, however, is completely reversed. As shown in Figure 2d, the higher the autothermal temperature of the feed to the reformer, the lower the net hydrogen yield. For example, at the S/C feed ratio of 2 mol/mol, the net hydrogen yield is 14.43 at the upper feed temperature 740.34 K, whereas it is 14.59 at the middle feed temperature of 702.15 K and 14.64 at the lower feed temperature of 687.99 K. This reverse relationship between the net hydrogen yield and the autothermal circulating feed temperature is due to the carbon formation−burning process in this autothermal system. Steam reforming extracts hydrogen not only from hydrocarbons but also from steam, whereas carbon formation extracts hydrogen only from hydrocarbons. Therefore, the greater the extent of hydrocarbon cracking for carbon formation, the higher the carbon generation, the higher the autothermal circulating feed temperature, and the lower the net hydrogen yield. According to bifurcation theory,[29] only the lower and upper steady states are stable, and the middle steady state is an unstable saddle-type state. When the S/C feed ratio is below 1.444 mol/mol, only one stable steady state exists in the reactor−regenerator system. Because a low S/C feed ratio (<1.444 mol/mol) is fed in this region, the extent of steam reforming becomes small. On the other hand, carbon formation and deposition compete for the reactant heptane. The greater the amount of carbon deposited, the higher the heat generation. As a result, the autothermal temperature of the feed circulating to the reformer is higher. If the S/C feed ratio is below 1.1475 mol/mol, the autothermal circulating feed temperature is very high, leading to thermal runaway (Figure 2a). In this investigation, the maximum net hydrogen yield is about 15.58 mol of hydrogen per mole of heptane fed at the lower steady state when the steam-to-carbon feed ratio is very close to the bifurcation point of 1.444 mol/mol. This is about 70.82% of the maximum theoretical hydrogen yield of 22 when the final steam reforming products are carbon dioxide and hydrogen.

Effect of the Efficiency of the Catalyst Regenerator. In the previous section, we assumed the efficiency of catalyst regenerator to be 100% for all reactions. In this section, to investigate the effects of heat generation from the catalyst regenerator on the overall performance of the autothermal CFB reformer, we simply assume different efficiencies for the catalyst regenerator and then calculate the heat generation required to preheat the cold feed water, heptane, and recycle catalyst. The exit gases from the catalyst regenerator are used for dry reforming in a novel dry reformer,[28] and the remaining carbon on the catalyst is recycled to the riser reformer. The S/C feed ratio is 2 mol/mol for this investigation. Figure 3a−d shows the bifurcation behavior when the efficiency of the catalyst regenerator is used as the bifurcation parameter. There are multiple steady states when the efficiency of the catalyst regenerator is higher than 81.5%. The autothermal temperatures of the feed circulating to the reformer, the carbon deposition rates, and the conversions of heptane are highest (or lowest) at the upper (or lower) steady states. However, the net hydrogen yields are lowest (or highest) at the upper (or lower) steady states. For example, when the efficiency of the catalyst regenerator is 0.9, the carbon deposition rates are 0.769, 1.026, and 1.314 kg/h at the lower, middle, and upper steady states, respectively (with corresponding autothermal feed temperatures of 686.9, 705.8, and 731.9 K). The net hydrogen yields are 13.955, 13.902, and 13.807 mol of hydrogen per mole of heptane fed, respectively. Because a highly efficient catalyst regenerator generates more heat of reaction from the burning of unreacted heptane and the byproducts methane, carbon monoxide, and carbon, the autothermal circulating feed temperature increases when the efficiency of catalyst regenerator increases. As in the previous case, the higher the autothermal feed temperature, the higher the carbon deposition rate in the bed. Because a highly efficient catalyst regenerator supplies more heat for endothermic steam reforming, the extent of the steam reforming of heptane and byproduction of methane increases. As a result, the conversion of heptane and the net hydrogen yield increase when the efficiency of the catalyst regenerator increases.

Bifurcation Behavior When Catalyst Regeneration Is after Gas−Solid Separation. In the following sections, the bifurcation behavior when catalyst regeneration occurs after gas−solid separation is investigated. As shown in Figure 1b, to produce pure hydrogen efficiently, the gas and solid mixture exiting from the riser reformer also first enters an exit hydrogen separator for the further removal of any remaining hydrogen before gas−solid separation and catalyst regeneration. Only the burning of carbon in the catalyst regenerator supplies the heat for the endothermic steam reforming of hydrocarbons in the riser reformer, whereas the separated gases from the gas−solid separator are used directly in downstream dry reforming in a novel dry reformer.[28] The simulation parameters and reaction conditions are the same as in the previous configuration, except that the base value of the steam-to-carbon feed ratio is reduced from 2 to 1 mol/mol.

Effects of the Steam-to-Carbon Feed Ratio. First, the effects of the steam-to-carbon feed ratio on the overall CFB autothermal reformer are investigated. The

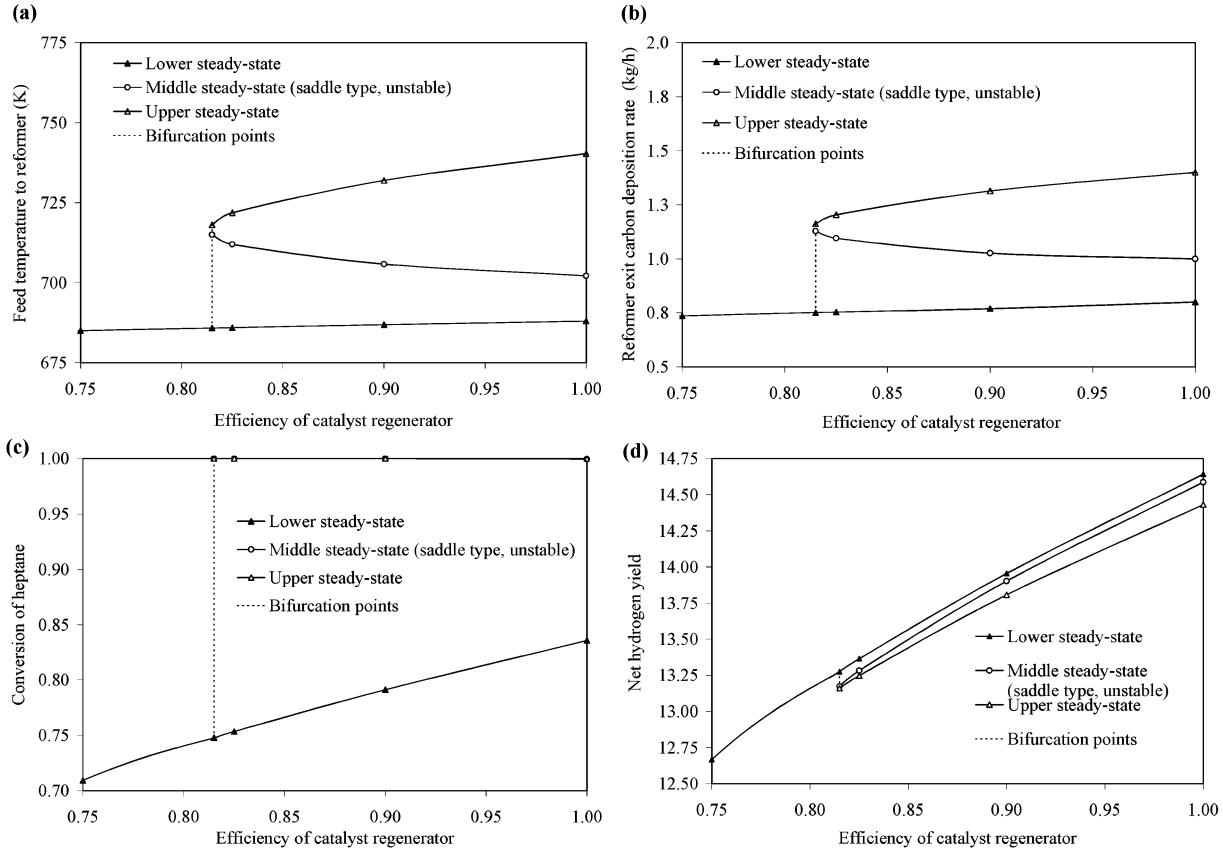

Figure 3. Bifurcation behavior with the efficiency of the catalyst regenerator as the bifurcation parameter in the autothermic CFB membrane reformer when catalyst regeneration is before gas−solid separation.

other standard parameters and reaction conditions for the bifurcation behavior investigation are listed in Table 3. Figure 4a−d shows the bifurcation behavior when the steam-to-carbon feed ratio is the bifurcation parameter. For this configuration, there are also three steady states in the autothermal CFB membrane reformer when the S/C feed ratio is between 0.994 and 1.023 mol/mol. Similarly, according to the magnitudes of the autothermal temperatures of the feed circulating to the reformer, we refer to them as the lower, middle, and upper steady states. The burning of carbon is the only heat source for endothermic steam reforming in the reformer. To keep the CFB membrane reformer operating under autothermal conditions, the carbon formation and deposition rate is larger than in the first configuration where the catalyst regeneration is before the gas−solid separation. Thus, for steady-state autothermal operation, the S/C feed ratio is lower than that of the previous configuration. The standard S/C feed ratio is reduced from 2 to 1 mol/mol.

Figure 4a shows that the autothermal temperature of the feed circulating to the reformer increases when the steam-to-carbon feed ratio increases. In contrast, Figure 4b shows that the carbon deposition rate increases slightly from the S/C feed ratio of 0.975 mol/mol to the multiplicity zone and then decreases when the S/C feed ratio extends beyond the right bifurcation point with the S/C feed ratio of 1.023 mol/mol. The conversion of heptane is always 100% (Figure 4c). The net hydrogen yield increases to the multiplicity region from the S/C feed ratio of 0.975 mol/mol. The net hydrogen yield is almost constant when the S/C feed ratio is between 1.023 and 1.05 mol/mol. In the multiplicity region, where S/C feed ratio is between 0.994 and 1.023 mol/mol, the carbon deposition rate at the lower steady state (the lowest temperature of feed circulating to the reformer) is the highest among these three steady states. In addition, the carbon deposition rates at the upper steady state (the highest temperatures of feed circulating to the reformer) are lowest among these three steady states, whereas the net hydrogen yields at the middle steady states are the highest. For example, around the S/C feed ratio of 1.02 mol/mol, the highest net hydrogen yield at the middle steady state is about 14.41 mol of hydrogen per mole of heptane fed, whereas at the high- and low-temperature steady states, the net hydrogen yields are 14.35 and 14.26 mol of hydrogen per mole of heptane fed, respectively. The order of the net hydrogen yield in the multiplicity region, from high to low, is middle, upper, and lower steady states. This behavior is quite different from that observed in the first case when catalyst regeneration occurs before gas−solid separation.

Because the minimum stoichiometric coefficient of steam to carbon (of heptane) is 1 when the final products of the steam reforming of heptane are carbon monoxide and hydrogen, the tendency for carbon formation increases when the steam feed is not sufficient (or when the S/C feed ratio is below 1 mol/mol). Thus, at low S/C feed ratios, for example, 0.975−0.994 mol/mol, the amount of carbon deposited is enough to keep the CFB membrane reformer operating autothermally, but the temperature of feed circulating to the reformer is not high. When the S/C feed ratio is higher than 1.023 mol/mol, the conversion of heptane is 100% in the reformer, and thus, there is no further carbon formation from heptane. In addition, because the use of a hydrogen permselective membrane enhances the reversible steam

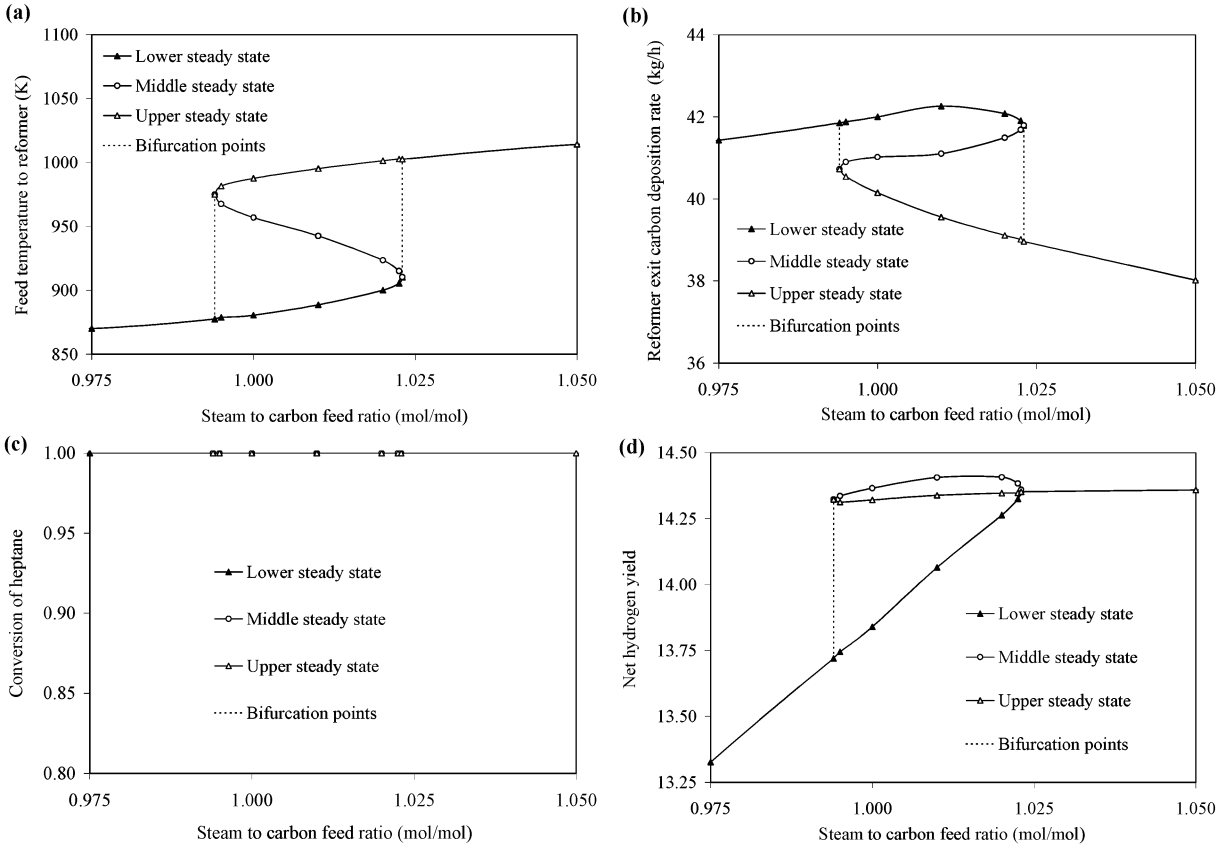

Figure 4. Bifurcation behavior with the steam-to-carbon feed ratio as the bifurcation parameter in the autothermic CFB membrane reformer when catalyst regeneration is after gas−solid separation.

reforming of the byproduct methane and the water−gas shift reaction, the contents of methane and carbon monoxide are usually very low in the reformer. Thus, the total carbon formation rate is low. On the other hand, carbon gasification, especially by oxygen, is significant because the oxygen permeation flux is high at high temperatures. The exothermic carbon oxidation by oxygen also supplies part of the heat for the endothermic reforming reactions in the reformer. As a result, under autothermal operation, the autothermal circulating feed temperature increases, and the carbon deposition rate decreases when the S/C feed ratio is higher than 1.023 mol/mol. Because steam reforming extracts hydrogen not only from hydrocarbons but also from steam, whereas carbon formation extracts hydrogen only from hydrocarbons, the higher the carbon deposition rate, the lower the net hydrogen yield. Although the carbon deposition rates at the middle steady states are higher than those at the upper steady states, the net hydrogen yields at the middle steady states are still higher than those at the upper steady states. For example, when the S/C feed ratio is 1.02 mol/mol, the carbon deposition rates are 42.08, 41.49, and 39.11 kg/h at the lower, middle, and upper steady states, respectively, whereas the corresponding net hydrogen yields are 14.26, 14.41, and 14.35 mol of hydrogen per mole of heptane fed. This phenomenon is due to the high circulating feed temperature at the upper steady state, making the water−gas shift reaction unfavorable for hydrogen production.

It seems that, at this preliminary stage of investigation, the implications of the second configuration under autothermal operation are quite complex. Furthermore, Figure 4 shows that the operating range of the S/C feed ratio parameter is very narrow (0.994−1.023 mol/mol) for bifurcation behavior. For practical operation, accurate control of the S/C feed ratio is very important.

Effect of the Efficiency of the Catalyst Regenerator. In the previous case for this second configuration, we assumed the efficiency of catalyst regenerator to be 100% for the burning of carbon. In this section, we investigate the effect of the efficiency of the catalyst regenerator on the overall performance of this TGR. We also simply assume different efficiencies for the catalyst regenerator and then calculate the heat generation required to preheat the cold feed water, heptane, and hot recycle catalyst. The exit gases from the catalyst regenerator are used for dry reforming in the novel dry reformer,[28] and the remaining carbon on the catalyst is recycled to the riser reformer. The S/C feed ratio is 1 mol/mol for this investigation.

Figure 5a−d shows the bifurcation behavior when the efficiency of the catalyst regenerator is used as a bifurcation parameter. The conversion of heptane is also 100% for the entire range of catalyst regeneration efficiencies covered (Figure 5c). There are three steady states when the efficiency of catalyst regenerator is higher than 96%. The autothermal temperature of the feed circulating to the reformer and the carbon deposition rate decrease when the efficiency of the catalyst regenerator increases, whereas the net hydrogen yield increases. For example, when the efficiency of the catalyst regenerator is 0.8, the autothermal temperature of the feed circulating to the reformer is 1037.5 K, the exit carbon deposition rate in the reformer is 45.49 kg/h, and the net hydrogen yield is 13.65 mol of hydrogen per mole of heptane fed. When the efficiency of the catalyst regenerator is increased to 0.9, the autothermal

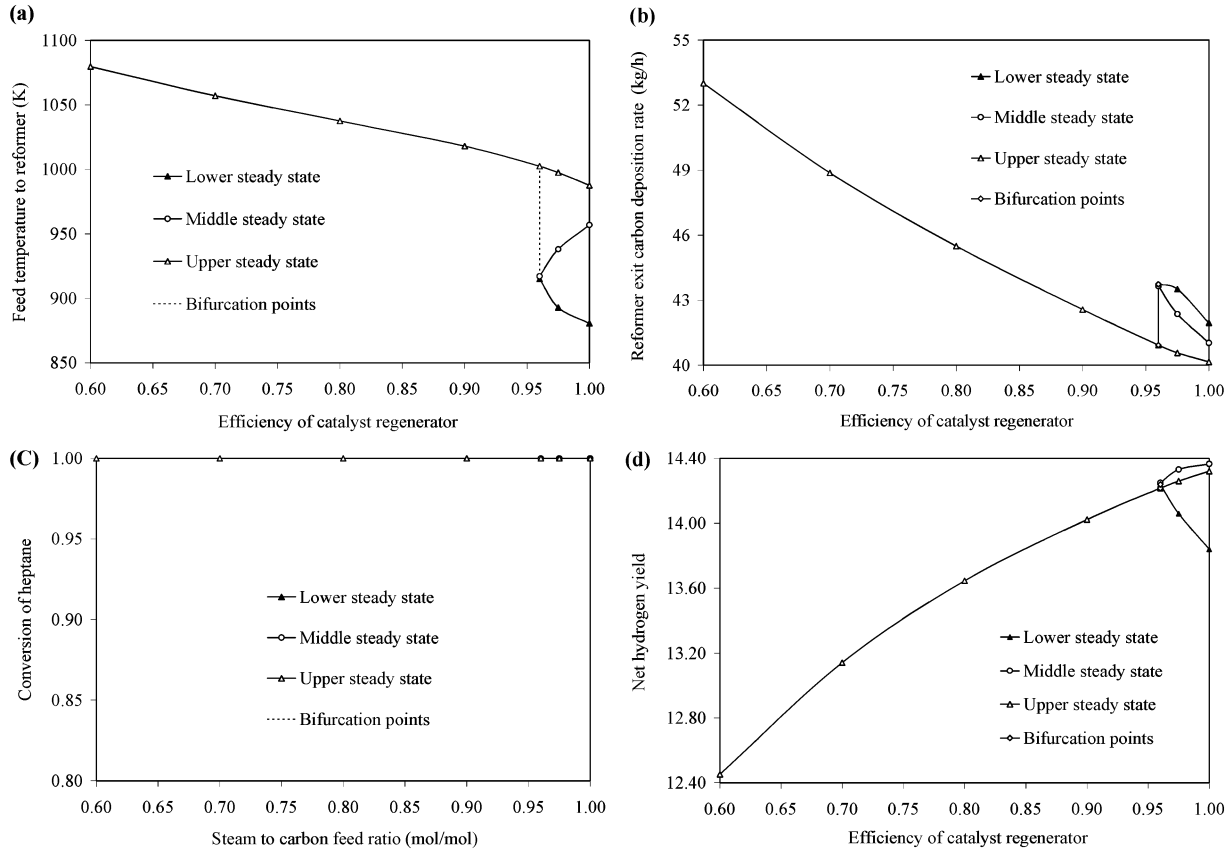

Figure 5. Bifurcation behavior with the efficiency of the catalyst regenerator as the bifurcation parameter in the autothermic CFB membrane reformer when catalyst regeneration is after gas−solid separation.

temperature of the feed circulating to the reformer decreases to 1017.97 K, the exit carbon deposition rate in the reformer also decreases to 42.57 kg/h, and the net hydrogen yield increases to 14.02 mol of hydrogen per mole of heptane fed. This is due to the fact that, when the catalyst regeneration efficiency increases, more heat is generated by the burning of the deposited carbon in the regenerator. Thus, the portion of heptane for carbon formation decreases, and the extent of the endothermic steam reforming reaction increases. As a result, the autothermal circulating feed temperature decreases, which, in turn, decreases the carbon formation rate in the bed. Because the extent of the endothermic steam reforming of hydrocarbons (heptane and byproduct methane) is enhanced when the catalyst regenerator efficiency is high, more hydrogen is produced, and the net hydrogen yield increases. In the multiplicity region (where the efficiency of the catalyst regeneration is >0.96), as in the previous case for this configuration, the carbon deposition rates at the lower (or upper) steady states are highest (or lowest) one among these three steady states, whereas the net hydrogen yields at the middle steady states is highest. For example, when the efficiency of the catalyst regenerator is 0.975, the carbon deposition rates are 43.50, 42.36, and 40.56 kg/h at lower, middle, and upper steady states, respectively, whereas the corresponding net hydrogen yields are 14.06, 14.33, and 14.26 mol of hydrogen per mole of heptane fed.

As in the previous case, Figure 5 also shows that the range of catalyst regenerator efficiency for the bifurcation behavior is very narrow (0.96−1.00). For practical operation, the catalyst regenerator can be overdesigned for high efficiency.

Conclusions

A preliminary bifurcation investigation has been carried out for the TGR formed from a novel CFB autothermal reformer using the S/C feed ratio and catalyst regenerator efficiency as bifurcation parameters. This study is a prelude to an experimental investigation of this novel reformer by an interdisciplinary research team. Two possible configurations for catalyst regeneration have been explored. For the first configuration with catalyst regeneration before gas−solid separation, there are three steady states when the S/C feed ratio is in the range of 1.444−2.251 mol/mol. Among these three steady states, the net hydrogen yields are highest at the lower-temperature steady states, whereas the carbon deposition rates at the upper steady states are the highest. For the second configuration with catalyst regeneration after gas−solid separation, there are also three steady states when the S/C feed ratio is in the range of 0.994−1.023 mol/mol. Among these three steady states, the net hydrogen yields are highest at the middle-temperature steady states, and the carbon deposition rates are highest at the lower-temperature steady states. The implications of this bifurcation behavior are analyzed and discussed. For both configurations, the net hydrogen yields increase with increasing catalyst regenerator efficiency because of the high heat generation and supply for the endothermic steam reforming in the riser reformer. In this preliminary investigation, the maximum net hydrogen yield is achieved in the first configuration; it is about 15.58 mol of hydrogen per mole of heptane fed at the lower steady state when the steam-to-carbon feed ratio is very close to the bifurcation point of 1.444 mol/

mol. These preliminary results show that this novel autothermal CFB reformer can be a very efficient producer of hydrogen and that a bifurcation behavior analysis is essential for the design, control, and optimization of this TGR. The possible exploitation of the CFB configuration as an efficient catalytic reactor was brought to our attention few years ago by the work and continuous contact with Professor John Grace, to whom this special issue of *Ind. Eng. Chem. Res.* is dedicated.

Acknowledgment

This work was financially supported by Auburn University, Grant 2-12085.

Nomenclature

Symbols

a, b = control indices for the membrane fluxes of hydrogen and oxygen, respectively
A_f = free cross-sectional area of the reactor (m^2)
C_i = molar concentration of component i (mol/m^3)
C_k = concentration of coke deposited on the catalyst (g/g of catalyst)
C_{pcat} = specific heat of the solid catalyst {J/[(g of catalyst) K]}
C_{pi} = specific heat of component i [J/(mol K)]
d_{H_2} = outside diameter of the hydrogen permselective membrane tubes (m)
d_{O_2} = outside diameter of the oxygen permselective membrane tubes (m)
DEN = term given in Table 1
E_{H_2} = activation energy for hydrogen permeation (J/mol)
E_{O_2} = activation energy for oxygen permeation (J/mol)
$F_{H_2,P}$ = molar flow rate of hydrogen in the hydrogen permselective membranes (mol/s)
F_i = molar flow rate of component i (mol/s)
F_{i0} = molar feed flow rate of component i at the entrance of the reformer (mol/s)
F_{iexit} = molar exit flow rate of component i at the exit of the reformer (mol/s)
$F_{N_2,P}$ = molar flow rate of nitrogen in the oxygen permselective membranes (mol/s)
$F_{O_2,P}$ = molar flow rate of oxygen in the oxygen permselective membranes (mol/s)
$F_{SG,P}$ = molar flow rate of sweep gas (steam) in the hydrogen permselective membranes (mol/s)
G_{cat} = mass flow rate of catalyst (g/s)
$\Delta H°$ = enthalpy change or heat of combustion (J/mol)
ΔH_j = heat of reaction for the jth reaction (J/mol)
ΔH_{vap} = heat of vaporization (J/mol)
J_{H_2} = permeation flux of hydrogen [$mol/(m^2\ s)$]
J_{O_2} = permeation flux of oxygen [$mol/(m^2\ s)$]
k_j = generalized (forward) reaction rate constant for the jth (reversible) reaction
K_i = absorption constant of component i
K_j = reaction equilibrium constant of the jth reaction
l = length of the reactor (m)
N_{H_2} = number of hydrogen permselective membrane tubes
N_{O_2} = number of oxygen permselective membrane tubes
P = reaction pressure (kPa)
P_i = partial pressure of component i (kPa)
$P_{H_2,P}$ = partial pressure of hydrogen in the hydrogen permselective membranes (kPa)
$P_{H_2,r}$ = partial pressure of hydrogen in the reformer reaction side (kPa)
$P_{O_2,P}$ = partial pressure of oxygen in the oxygen permselective membranes (kPa)
$P_{O_2,r}$ = partial pressure of oxygen in the reformer reaction side (kPa)
$\dot{Q}$ = rate of heating along the reactor length [J/(s m)]
Q_g = rate of heat generated (J/s)
Q_{H_2} = preexponential factor for the hydrogen permeation flux
Q_{O_2} = preexponential factor for the oxygen permeation flux
Q_P = preheating rate (J/s)
r_j = generalized rate of reaction j {mol/[(g of catalyst) s]}
r_{j0} = generalized rate of reaction j with fresh catalyst {mol/[(g of catalyst) s]}
R = gas constant [8.314 J/(mol K)]
T = temperature (K)
T_{exit} = riser reformer exit temperature (K)
T_0 = autothermal feed temperature (K)
T' = mixing temperature of steam, heptane, and recycled catalyst after preheating (K)
T_{room} = room temperature (K)

Greek Letters

α_C = deactivation constant (gcatalyst/gcoke)
δ_i = thickness of hydrogen or oxygen membranes (i = H_2,O_2) (m)
ϵ = void fraction
ρ_c = density of catalyst (kg/m^3)
$\sigma_{i,j}$ = stoichiometric coefficient of component i in the jth reaction
ϕ = catalyst activity function

Literature Cited

(1) Goltsov, V. A.; Nejat Veziroglu, T. A Step on the Road to Hydrogen Civilization. *Int. J. Hydrogen Energy* **2002**, *27* (7−8), p719−723.

(2) Ohi, J. Hydrogen Energy Futures: Scenario Planning by the U.S. DOE Hydrogen Technical Advisory Panel. Presented at the 14th World Hydrogen Energy Conference, Montreal, Canada, Jun 9−13, 2002.

(3) Tottrup P. B. Evaluation of Intrinsic Steam Reforming Kinetic Parameters from Rate Measurements on Full Particle Size. *Appl. Catal.* **1982**, *4*, 377−389.

(4) Xu, J.; Froment, G. F. Methane Steam Reforming, Methanation and Water−Gas Shift: I. Intrinsic Kinetics. *J. AIChE* **1989**, *35* (1), 88−96.

(5) Elnashaie, S. S. E. H.; Elshishini, S. S. *Modelling, Simulation and Optimization of Industrial Fixed Bed Catalytic Reactors*; Gordon and Breach Science Publishers: London, U.K., 1993.

(6) Christensen, T. S. Adiabatic Prereforming of Hydrocarbons—An Important Step in Syngas Production. *Appl. Catal. A: Gen.* **1996**, *138*, 285−309.

(7) Chen, Z.; Yan, Y.; Elnashaie, S. S. E. H. Modeling and Optimization of a Novel Membrane Reformer for Higher Hydrocarbons. *AIChE J.* **2003**, *49* (5), 1250−1265.

(8) Rostrup-Nielsen, J. Hydrogen via Steam Reforming of Naphtha, *Chem. Eng. Prog.* **1977**, *9*, 87.

(9) Elnashaie S. S. E. H.; Abashar, M. E.; Al-Ubaid, A. S. Simulation and Optimization of an Industrial Ammonia Reactor. *Ind. Eng. Chem. Res.* **1988**, *27*, 2015.

(10) Twigg, M. V. *Catalyst Handbook*, 2nd ed.; Wolfe Publishing Ltd.: London, 1989; 225−282.

(11) Dyer, P. N.; Chen, C. M. Engineering Development of Ceramic Membrane Reactor System for Converting Natural Gas to H_2 and Syngas for Liquid Transportation Fuel. In *Proceedings of the 1999 Hydrogen Program Review*; Report NREL/CP-570-26938; U.S. Department of Energy, U.S. Government Printing Office: Washington, DC, 1999.

(12) Dyer, P. N.; Chen, C. M. Engineering Development of Ceramic Membrane Reactor System for Converting Natural Gas to H_2 and Syngas for Liquid Transportation Fuel. In *Proceedings of the 2000 Hydrogen Program Review*; Report NREL/CP-570-28890; U.S. Department of Energy, U.S. Government Printing Office: Washington, DC, 2000; pp 1−11.

(13) Sammels, A. F.; Schwartz, M.; Mackay, R. A.; Barton, T. F.; Peterson, D. R. Catalytic Membrane Reactors for Spontaneous Synthesis Gas Production. *Catal. Today* **2000**, *56*, 325.

(14) Shah, M. M.; Drnevich, R. F. Integrated Ceramic Membrane System for Hydrogen Production. In *Proceedings of the 2000 Hydrogen Program Review*; Report NREL/CP-570-28890; U.S.

Department of Energy, U.S. Government Printing Office: Washington, DC, 2000; pp 1−6.

(15) Makel, D. Low Cost Microchannel Reformer for Hydrogen Production from Natural Gas. California Energy Commission (CEG), Energy Innovations Small Grant (EISG) Program, 1999. See http://eisg.sdsu.edu/shortsums/shortsum9914.htm.

(16) Hayakawa, T.; Andersen, A. G.; Shimizu, M.; Suzuki, K.; Takehira, K. Partial Oxidation of Methane to Synthesis Gas over Some Tibanates Based Perovskite Oxides. *Catal. Lett.* **1993**, *22*, 307−317.

(17) Theron, J. N.; Dry, M. E.; Steen, E.Van; Fletcher, J. C. G. Internal and External Transport Effects During the Oxidative Reforming of Methane on a Commercial Steam Reforming Catalyst. *Stud. Surf. Sci. Catal.* **1997**, *107*, 455−460.

(18) Elnashaie S. S. E. H; Adris, A. M. A Fluidized Bed Steam Reformer for Methane. In *Proceedings of the VI International Fluidization Conference, Banff, Canada*; Grace, J., Shemilt, L. W., Bergougnou, M. M., Eds.; AIChE Publications: New York, 1989; p 319.

(19) Adris, A. M.; Elnashaie, S. S. E. H.; Hughes, R. A Fluidized Bed Membrane Reactor for the Steam Reforming of Methane. *Can. J. Chem. Eng.* **1991**, *69* (10), 1061.

(20) Adris, A.; Grace, J.; Lim, C.; Elnashaie, S. S. E. H. Fluidized Bed Reaction System for Steam/Hydrocarbon Gas Reforming to Produce Hydrogen. U.S. Patent 5,326,550, Jun 1994.

(21) Adris, A. M.; Lim, C. J.; Grace, J. R. The Fluidized Bed Membrane Reactor (FBMR) System: A Pilot Scale Experimental Study. *Chem. Eng. Sci.* **1994**, *49*, 5833.

(22) Adris, A. M.; Lim, C. J.; Grace, J. R. The fluidized-Bed Membrane Reactor for Steam Methane Reforming: Model Verification and Parametric Study. *Chem. Eng. Sci.* **1997**, *52* (10), 1609.

(23) Adris, A.; Grace, J.; Lim, C.; Elnashaie, S. S. E. H. Fluidized Bed Reaction System for Steam/ Hydrocarbon Gas Reforming to Produce Hydrogen. Canadian Patent 2,081,170, Dec 2002.

(24) Roy, S.; Pruden, B. B.; Adris, A. M.; Lim, C. J.; Grace, J. R. Fluidized-Bed Steam Methane Refroming with Oxygen Input. *Chem. Eng. Sci.* **1999**, *54*, 2095−2102.

(25) Chen, Z.; Elnashaie, S. S. E. H. Efficient Production of Hydrogen from Higher Hydrocarbons using Novel Membrane Reformer. Presented at the 14th World Hydrogen Energy Conference, Montreal, Canada, Jun 9−13, 2002.

(26) Chen, Z.; Yan, Y.; Elnashaie, S. S. E. H. Using Coking and Decoking Model in a Circulating Fast Fluidized Bed Membrane Reformer for Efficient Production of Pure Hydrogen by Steam Reforming of Higher Hydrocarbons. In *Proceedings of the Regional Symposium on Chemical Engineering and the 16th Symposium of Malaysian Chemical Engineers*; University of Malaya Press: Kuala Lumpur, Malaysia, 2002; pp 1239−1247.

(27) Chen, Z.; Yan, Y.; Elnashaie, S. S. E. H. Novel Circulating Fast Fluidized Bed Membrane Reformer for Efficient Production of Hydrogen from Steam Reforming of Methane. *Chem. Eng. Sci.* **2003**, *58* (19), 4335−4349.

(28) Prasad, P.; Elnashaie, S. S. E. H. Novel Circulating Fluidized Bed Membrane Reformer for the Efficient Production of Ultraclean Fuels from Hydrocarbons. *Ind. Eng. Chem. Res.* **2002**, *41*, 6518−6527.

(29) Elnashaie, S. S. E. H.; Elshishini, S. S. *Dynamic Modeling, Bifurcation and Chaotic Behavior of Gas−Solid Catalytic Reactors*; Gordon and Breach Science Publishers: London, 1996.

(30) Siminski. V. J.; Wright, F. J.; Edelman, R. B.; Economos, C.; Fortune, O. F. *Research on Methods of Improving the Combustion Characteristics of Liquid Hydrocarbon Fuels*; Report AFAPL TR 72−74; Air Force Aeropropulsion Laboratory: Wright Patterson Air Force Base, OH, 1972; Vols. I and II.

(31) Jin, W.; Gu, X.; Li, S.; Huang, P.; Xu, N.; Shi, J. Experimental and Simulation Study on a catalyst Packed Tubular Dense Membrane Reactor for Partial Oxidation of Methane to Syngas. *Chem. Eng. Sci.* **2000**, *55*, 2617−2625.

(32) Rostrup-Nielsen, J. R. Coking on Nickel Catalysts for Steam Reforming of Hydrocarbons. *J. Catal.* **1974**, *33*, 184−201.

(33) Snoeck, J. W.; Froment, G. F.; Fowles, M. Kinetic study of the Carbon Filament Formation by Methane Cracking on a Nickel Catalyst. *J. Catal.* **1997**, *169*, 250−262.

(34) Tottrup, P. B. Kinetics of Decomposition of Carbon Monoxide on a Supported Nickel Catalyst. *J. Catal.* **1976**, *42*, 29−36.

(35) Chen, C. X.; Horio, M.; Kojima, T. Numerical Simulation of Entrained Flow Coal Gasifiers. Part I: Modeling of Coal Gasification in an Entrained Flow Gasifier. *Chem. Eng. Sci.* **2000**, *55*, 3861−3874.

(36) Patience, G. S.; Chaouki, J.; Berruti, F.; Wong, R. Scaling considerations for circulating fluidized bed risers. *Powder Technol.* **1992**, *72* (1), 31−37.

(37) Kunii, D.; Levenspiel, O. Circulating Fluidized-Bed Reactors. *Chem. Eng. Sci.* **1997**, *15*, 2471−2484.

(38) Shu, J.; Grandjean, B. P. A.; Kaliaguine, S. Methane Steam Reforming in Asymmetric Pd− and Pd−Ag/porous SS Membrane Reactor. *Appl. Catal. A* **1994**, *119*, 305−325.

(39) Tsai, C. Y.; Dixon, A. G.; Moser, W. R.; Ma, Y. H. Dense Perovskite Membrane Reactors for Partial Oxidation of Membrane to Syngas. *J. AIChE* **1997**, *43* (11A), 2741.

(40) Ritchie J. T.; Richardson, J. T.; Luss, D. Ceramic Membrane Reactor for Synthesis Gas Production. *J. AIChE* **2001**, *47* (9), 2092−2100.

(41) Kunii, D.; Levenspiel, O. Entrainment of Solids from Fluidized Beds: I. Hold-Up of Solids in the Freeboard, II. Operation of Fast Fluidized Beds. *Powder Technol.* **1990**, *61*, 193−206.

Received for review October 12, 2003
Revised manuscript received December 20, 2003
Accepted January 5, 2004

IE0341799